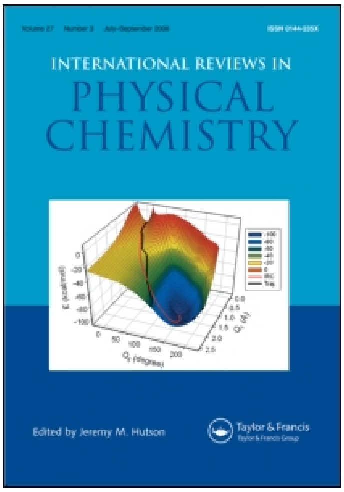

International Reviews in Physical Chemistry
Publication details, including instructions for authors and subscription information:
http://www.informaworld.com/smpp/title~content=t713724383

Infrared Investigations of Negatively Charged Complexes and Clusters

D. A. Wild[a]; E. J. Bieske[a]
[a] School of Chemistry, University of Melbourne, Parkville, Victoria, Australia

To cite this Article Wild, D. A. and Bieske, E. J.(2003) 'Infrared Investigations of Negatively Charged Complexes and Clusters', International Reviews in Physical Chemistry, 22: 1, 129 — 151

To link to this Article: DOI: 10.1080/0144235021000060165

URL: http://dx.doi.org/10.1080/0144235021000060165

Int. Reviews in Physical Chemistry, 2003
Vol. 22, No. 1, 129–151

Infrared Investigations of Negatively Charged Complexes and Clusters

D. A. WILD and E. J. BIESKE*
School of Chemistry, University of Melbourne, Parkville, Victoria 3010, Australia

The review describes recent progress in the characterization of size-selected negatively charged clusters in the gas phase using vibrational predissociation spectroscopy. Examples from the authors' laboratory are used to demonstrate the way in which spectra are obtained and interpreted to provide information on anion–neutral interactions. Infrared studies of simple dimer complexes consisting of hydrogen molecules attached to halide anions (Cl^-–H_2, Br^-–H_2, I^-–H_2) are described. From rotationally resolved spectra in the 2.5 μm H–H stretch region one can deduce that the complexes have linear equilibrium structures and can ascertain intermolecular separations. Corresponding spectra of the Cl^-–D_2 and Br^-–D_2 isotopomers display a series of clearly resolved doublets, highlighting the importance of hindered internal rotation of the D_2 subunit. Studies of Cl^-–$(C_2H_2)_n$, Br^-–$(C_2H_2)_n$ and I^-–$(C_2H_2)_n$ clusters containing up to nine C_2H_2 molecules illustrate how infrared spectra can be used to explore the progressive 'solvation' of halide anions. The smaller clusters ($n \leq 6$) have morphologies in which equivalent acetylene molecules are hydrogen bonded to the interior halide anion. For $n > 6$ there is evidence for structures in which one or more acetylene molecules are situated in the second solvation shell and also for the existence of multiple isomeric forms. The article concludes by discussing prospects for extending spectroscopic studies to hitherto uncharacterized anion complexes.

Contents

---

* E-mail: evanjb@unimelb.edu.au

International Reviews in Physical Chemistry ISSN 0144–235X print/ISSN 1366–591X online © 2003 Taylor & Francis Ltd
http://www.tandf.co.uk/journals
DOI: 10.1080/0144235021000060165

1. Introduction

This article describes recent advances in the characterization of negatively charged complexes and clusters using infrared spectroscopy. The anion species under consideration are analogues of neutral van der Waals molecules which, for almost 30 years, have been studied through their absorptions in the microwave, infrared, visible, and UV portions of the electromagnetic spectrum [1–9]. Corresponding spectroscopic studies of charged complexes and clusters, which began in the 1980s for cations [10–12] and in the 1990s for anions [13–16], have been driven by a desire to understand the cohesive forces acting between ions and neutral molecules. Interactions between solute ions and neutral solvent molecules govern the structural and energetic properties of electrolyte solutions and also their dynamical behaviour (ion conductivities and solvent relaxation times). Ion–solvent interactions also play a decisive role in determining the secondary and tertiary structures of larger biological molecules, which are vital for their function.

Laboratory investigations of neutral van der Waals molecules and ionic complexes and clusters have quite different histories. For neutral complexes and clusters, the primary source of information has conventionally been spectroscopy in the microwave, infrared, visible or UV parts of the electromagnetic spectrum. Indeed, usually the only way to infer the existence of a neutral van der Waals molecule is to obtain and analyse its spectrum. High-resolution spectra provide relatively direct links to quantitative details of intermolecular potential energy surfaces [1–7, 9]. Lower-resolution spectra displaying vibrational or vibronic features have proved useful for distinguishing between different isomeric forms of complexes and clusters, since the vibrational frequencies and intensities of the 'solvent' and 'solute' molecules depend sensitively on their local environment [8].

Traditionally, the investigation of ionic complexes has been the province of mass spectroscopists, since by using mass spectrometry charged complexes and clusters can be securely identified in the gas phase even when they are present in extremely low concentrations. Several decades ago it was discovered that gas–phase ions tended to cluster together with molecules present in surrounding gas [17–19]. This realization was followed by a series of measurements of clustering equilibria:

$$A^{\pm}\text{–}L_n + L \rightleftharpoons A^{\pm}\text{–}L_{n+1}$$

where $A^{\pm}$ is an atomic or molecular ion and L is a 'solvent' atom or molecule. Measurements of the equilibrium constant over a range of temperatures allow van't Hoff plots to be constructed from which solvent binding enthalpies and entropies can be ascertained. After more than 30 years of measurements, the database for the energetics of gaseous ion clusters is vast. The *NIST WebBook* [20] includes a compilation of binding enthalpies and entropies for thousands of ion–neutral complexes and clusters (data for more than 200 clusters containing the F^- anion alone are listed). Despite being an excellent source of thermochemical data, the ion–ligand clustering studies provide limited structural information, although abrupt

Table 1. Anion complexes and clusters characterized using infrared spectroscopy. The clusters can be divided into three classes: hydrogen-bonded complexes, S_N2 complexes and solvated electron clusters. For each class, the complexes are roughly ordered according to the complexity of the 'solvent' molecules. With the exceptions of Cl^-–$(CH_3Cl)_n$ and Br^-–$(CH_3Br)_n$, the studies have concentrated on exciting hydrogen stretch vibrations in the 2500–4000 cm^{-1} range.

Complex	Comments	References
Hydrogen bonded		
F^-–$(D_2)_n$	To $n = 6$	[22]
Cl^-–$(H_2)_n$	To $n = 3$; rotational resolution for Cl^-–H_2 and Cl^-–D_2	[22–24]
Br^-–H_2	rotational resolution for Br^-–H_2 and Br^-–D_2	[25, 26]
I^-–H_2	rotational resolution	[26]
F^-–$(H_2O)_n$	To $n = 5$	[15, 27]
Cl^-–$(H_2O)_n$	To $n = 5$	[27–32]
Br^-–$(H_2O)_n$	To $n = 6$	[27, 29, 30, 33, 34]
I^-–$(H_2O)_n$	To $n = 6$; partial rotational resolution for I^-–HDO	[13, 14, 29, 30, 33–36]
O_2^-–$(H_2O)_n$	To $n = 6$	[37, 38]
OH^-–$(H_2O)_n$	To $n = 5$	[39]
SO_2^-–H_2O	Double H bond	[40]
Cl^-–$(C_2H_2)_n$	To $n = 9$	[41]
Br^-–$(C_2H_2)_n$	To $n = 8$; partial rotational resolution for Br^-–C_2H_2	[42, 43]
I^-–$(C_2H_2)_n$	To $n = 4$	[16]
Cl^-–NH_3		[44]
I^-–CH_3	Open shell	[45]
Br^-–CH_2Br	Open shell	[45]
F^-–$(CH_4)_n$	Partial rotational resolution	[46]
Cl^-–$(CH_4)_n$	Partial rotational resolution	[47]
Br^-–$(CH_4)_n$	Partial rotational resolution	[46]
I^-–HCOOH	Double H bond	[48]
Cl^-–$(CH_3OH)_n$	Up to $n = 12$	[49]
I^-–$(CH_3OH)_n$	Up to $n = 2$	[50, 51]
I^-–C_2H_5OH		[50]
I^-–C_3H_7OH		[50]
S_N2		
Cl^-–CH_3Br	Partial rotational resolution	[52]
Cl^-–$(CH_3Cl)_n$	925–1090 cm^{-1}	[53]
Br^-–$(CH_3Br)_n$	925–1090 cm^{-1}	[53]
Solvated electron		
$(H_2O)_n^-$	Hydrated electron clusters	[54–56]

changes in binding energies and cluster abundances as a function of ligand number are often presumed to correspond to solvent shell closure [21].

Infrared investigations of gas-phase anion complexes were initiated by Okumura and coworkers in the 1990s with a study of the I^-–H_2O complex [13]. Since then more than 25 different anion cluster systems have been spectroscopically characterized. These are catalogued in table 1 (the list is reasonably comprehensive but is certain to be superseded). The majority of the complexes consist of 'solvent' molecules containing an X–H group (e.g. H_2, H_2O, C_2H_2, NH_3, CH_4, CH_3OH, C_2H_5OH) hydrogen bonded to a core anion (e.g. F^-, Cl^-, Br^-, I^-, O_2^-, SO_2^-). The hydrated-halide complexes and clusters, in particular, have been extensively studied because of their relevance to understanding aqueous solvation. The focus on hydrogen-bonded complexes is provoked not only by their significance to anion solvation in bulk media but also because the hydrogen stretch vibrations can be excited by light in the 3 μm region that is conveniently generated by an optical parametric oscillator or difference frequency mixing.

The intermolecular bonds in hydrogen-bonded anion complexes generally have strengths that are intermediate between those of van der Waals bonds between neutral molecules and strong covalent bonds ($10\,\mathrm{kJ\,mol^{-1}} < D_o < 80\,\mathrm{kJ\,mol^{-1}}$). Although a degree of molecular distortion inevitably accompanies formation of the intermolecular bond, in most cases the structural and chemical integrity of the anion core and the neutral solvent molecules is preserved. In some instances, such as the hydrated halide clusters (e.g. Cl^-–$(H_2O)_n$, Br^-–$(H_2O)_n$, I^-–$(H_2O)_n$), robust hydrogen bonds are also established between the ligands, so that the clusters have structures in which the halide anion is tethered to the surface of a hydrogen-bonded solvent network [30, 57]. For other clusters, strong hydrogen bonds between the ligands and the anion core prevent the ligands from establishing secondary hydrogen bonds with one another. This situation occurs for F^-–$(H_2O)_n$ and the halide–acetylene clusters (e.g. Cl^-–$(C_2H_2)_n$, Br^-–$(C_2H_2)_n$ and Br^-–$(C_2H_2)_n$), which are discussed later in section 4.2. An interesting case is SO_2^-–H_2O, where each hydrogen atom of the water molecule is attached by a hydrogen bond to one oxygen atom of the SO_2^- anion. This is achieved at the expense of bond angle distortion of the H_2O molecule [40].

In many instances, spectroscopic studies of anion complexes and clusters have been complemented by *ab initio* calculations that have yielded structural parameters (bond lengths, bond angles), vibrational frequencies and solvent binding energies [51, 56–63]. Correspondences between calculated and measured vibrational frequencies have regularly been used to distinguish different isomeric forms and to validate interpretations of experimental data. Connections between theory and experiment have played a particularly important role in interpreting infrared spectra of the hydrated halide [15, 57, 59, 64] and hydrated electron clusters [56]. *Ab initio* calculations on anions have been reviewed by Simons and Jordan [65].

The properties of negatively charged complexes and clusters have been elucidated using a number of experimental techniques besides infrared spectroscopy. We have already mentioned high-pressure mass spectrometry and its use in the determination of binding enthalpies and entropies. There are several reviews covering this work [17–19]. Photoelectron spectroscopy is another important method that has been used extensively to provide dissociation energies for anion–neutral intermolecular bonds [66–68]. This technique, which involves measuring the energies of electrons photodetached by a fixed-frequency laser beam, possesses the considerable advantage that it can be applied to almost any anion complex or cluster. Sudden declines in the bond energies are presumed to correspond to solvent shell completion. For example, by measuring the vertical electron detachment energies of O^-–Ar_n clusters, Bowen and coworkers were able to determine stepwise Ar solvent stabilization energies. From these they were able to deduce that the first solvation shell closes at $n = 12$ and that the larger clusters adopt polyicosahedral packing patterns [69]. A variant of photoelectron spectroscopy, with substantially better resolution (≈ 1–$2\,\mathrm{cm}^{-1}$), is zero electron kinetic energy (ZEKE) spectroscopy [70–73]. This method has proved capable of yielding spectra that can be interpreted to furnish empirical potential energy surfaces describing anion–neutral interactions as exemplified in recent studies of the $ArCl^-$, $KrBr^-$, $XeBr^-$ and $KrCl^-$ dimers [74, 75].

Molecular anions do not often possess stable excited electronic states lying below their detachment thresholds so negatively charged clusters usually cannot be characterized using electronic spectroscopy. However, bound–free electronic transitions of a diatomic halogen anion surrounded by several 'solvent' molecules (e.g. Br_2^-–Ar_n, I_2^-–Ar_n, I_2^-–$(CO_2)_n$) have been probed to investigate geminate recombination in a finite medium [76–79]. The formation of delicate dipole-bound anion complexes through electron transfer from Rydberg atoms to neutral van der Waals molecules has also been investigated [80, 81].

In the remainder of this article, we attempt to demonstrate how infrared spectroscopy can be deployed to yield structural information for anion complexes and clusters, concentrating on work undertaken in our own laboratory. After a brief examination of experimental approaches we discuss the Cl^-–H_2, Br^-–H_2 and I^-–H_2 dimers to show how rotationally resolved infrared spectra can be used to extract quantitative structural details [23–26]. Following this, we describe infrared studies of the Cl^-–$(C_2H_2)_n$, Br^-–$(C_2H_2)_n$ and I^-–$(C_2H_2)_n$ halide–acetylene clusters to illustrate the manner in which vibrationally resolved infrared spectra can be used to follow the progressive solvation of a core anion [16, 41–43].

2. Experimental approaches

2.1. *Vibrational predissociation spectroscopy*

Anion complexes and clusters represent challenging spectroscopic targets and it is only in recent years that appropriate experimental tools have been developed. Two obstacles must be surmounted. (1) Generally, it is difficult to create ion complexes in sufficient densities for the implementation of traditional spectroscopic approaches (e.g. direct infrared absorption spectroscopy). (2) In a plasma environment conducive to the formation of ions and ion clusters, there are usually a number of coexisting species whose infrared spectra may overlap. For this reason disentangling and assigning spectra can pose severe challenges.

An approach that is both *sensitive* and *mass selective* involves exposing ionic complexes to tuneable infrared light in a tandem mass spectrometer, with photoabsorption being inferred through the production of charged photofragments. The idea behind the scheme is illustrated in figure 1 with application to the Cl^-–H_2 complex. Tuneable IR light excites a high-frequency intramolecular vibration (in this case the H_2 stretch) localized on one component of the complex or cluster. Eventually, on a timescale that can range from picoseconds to milliseconds depending on the system, the vibrational energy migrates to the weak intermolecular bond causing its rupture and the liberation of charged and neutral fragments. A spectrum is obtained by monitoring the charged fragment anions as the infrared wavelength is scanned.

There are several benefits inherent in this form of VP spectroscopy. First of all, the use of detectors capable of sensing single ions confers exceptional sensitivity, rendering it feasible to investigate a range of exotic charged species that may be present only in low abundance. Secondly, mass selection of the parent cluster means

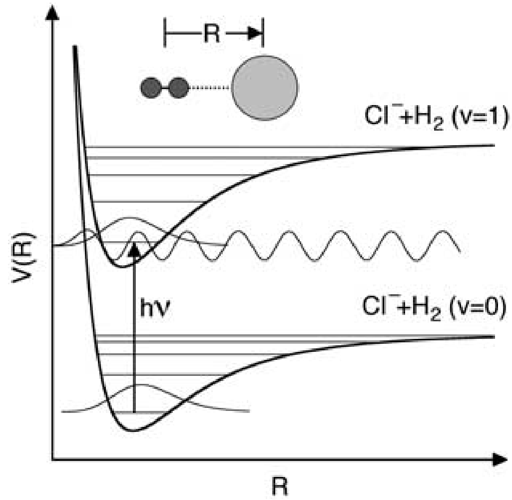

Figure 1. Strategy for obtaining infrared vibrational predissociation (VP) spectra of mass-selected anion complexes as applied to the Cl^-–H_2 dimer. The lower and upper potential energy curves correspond to Cl^-+H_2 ($v = 0$) and Cl^-+H_2 ($v = 1$) respectively. Absorption of an infrared photon with appropriate wavelength excites Cl^-–H_2 to a level supported by the Cl^-+H_2 ($v = 1$) curve. Coupling with the continuum associated with the lower Cl^-+H_2 ($v = 0$) potential leads to vibrational predissociation and liberation of Cl^- and H_2 ($v = 0$) fragments.

that there is usually little doubt about the identity of the absorbing species. As well, the second mass selection stage makes it possible to gauge the size distribution of fragment ions, which can be useful for estimating dissociation energies [82]. A significant advantage of the arrangement is that it is relatively straightforward to undertake spectroscopic studies of mass-selected clusters containing increasing numbers of solvent molecules to explore the first few solvation steps.

Probing ions by exposing them to tuneable light in a mass spectrometer apparatus has been employed for many years to study strongly bound molecular ions using microwave, infrared, visible and ultraviolet excitation [83–85]. Its application to the interrogation of weakly bound ionic complexes and clusters was pioneered by Okumura, Yeh and Lee in 1985 with studies of H_3^+–$(H_2)_n$ cation clusters [10]. Other groups have since used the technique to undertake infrared investigations of a large variety of cation complexes and clusters including proton-bound complexes [86, 87], metal–ligand complexes [88–90] and clusters containing aromatic molecules [91, 92]. The technique was first used by Okumura and coworkers to investigate anion complexes with a study of I^-–H_2O in 1996 [13].

One limitation of the VP technique is that it is only useful for probing transitions that terminate above the cluster's dissociation threshold since photon absorption is inferred from the production of fragment ions. Studies of cation complexes show that when the ligand's binding energy exceeds the energies of the cluster's fundamental vibrational modes it is sometimes possible to excite overtone or combination bands to promote dissociation. Alternatively, complexes containing a weakly bound 'spy' atom (ideally a rare gas atom) can be synthesized and probed. Vibrational excitation of the core anion complex leads to the loss of the 'spy' atom, producing a detectable anion fragment. This trick, initially devised to investigate protonated water clusters [93], has recently been used to great effect by Johnson and coworkers for probing many of the hydrated halide and hydrated electron anion complexes and clusters listed in table 1 [14, 55]. A second inherent problem with the VP approach is that the spectral lines are always lifetime broadened because the upper state levels are coupled to the dissociative continuum. The broadening can obscure rotational features in spectra of complexes that undergo very rapid predissociation, especially for larger species with small rotational constants.

2.2. *Apparatus*

In our studies, the VP scheme is instituted using the tandem mass spectrometer system illustrated in figure 2. The machine consists of an ion source, primary quadrupole mass filter for selection of the parent ion complexes, a radio–frequency octopole ion guide, a secondary quadrupole mass filter for selection of the photofragment and an ion detector. While travelling through the octopole guide, the ions meet a counterpropagating infrared light beam, which, when tuned to an appropriate wavelength, excites the complexes to predissociative vibrational levels. Resulting anion photofragments are mass selected by a second quadrupole mass filter and are subsequently sensed by a charged particle detector. Other mass selection arrangements have also been used for anion VP studies, most commonly time-of-flight mass spectrometers [13, 14].

In our apparatus the anion clusters are synthesized by bombarding a pulsed supersonic gas expansion with electrons (typical energy $\approx$500 eV). The gas cools as it expands adiabatically into the vacuum, reducing the temperature of the translational and rotational degrees of freedom to a few kelvins. The electron beam serves to ionize the gas and forms a cool micro-plasma, conducive to the formation of weakly bound ionic clusters and complexes. Halide anions (F^-, Cl^-, Br^-, I^-) are usually created through dissociative attachment of slow secondary electrons to appropriate precursor molecules (e.g. NF_3, CCl_4, CH_2Br_2, CH_3I) and combine with entrained neutral ligand molecules (e.g. H_2, H_2O, NH_3, C_2H_2) in the initial part of the expansion through three-body association reactions. Generally, the anion precursor molecules and the ligand molecules are seeded in an excess of Ar gas. While it might be expected that electron impact would heat the expanding gas, under appropriate conditions the infrared spectra are consistent with rotational temperatures as low as 30 K [25]. The low temperatures achieved in supersonic expansions are important not only for optimizing formation of the delicate negatively charged clusters but also for ensuring that the infrared spectra are not unduly congested by transitions from higher rotational and vibrational levels.

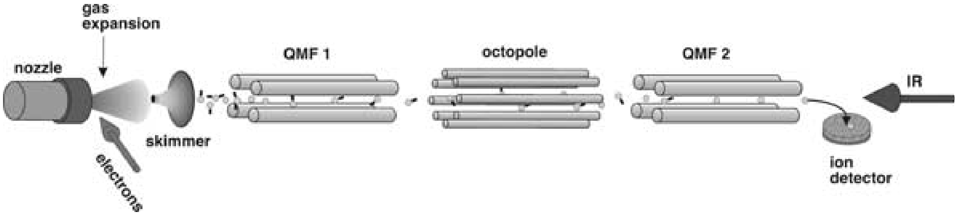

Figure 2. Tandem mass spectrometer apparatus used for spectroscopic investigations of negatively charged complexes and clusters. Electrostatic lenses link each stage, and the whole system is enclosed in a differentially pumped vacuum chamber.

Although most of the anion complexes listed in table 1 have been generated by crossing supersonic expansions of various gas mixtures with electron beams, other approaches have also been used. These include corona discharges [39], thermionic emission of halide ions from coated filaments [15], laser ablation [94], electron transfer from Rydberg atoms [80, 81] and laser excited photoelectron emission from a metal surface [95].

3. Simple systems: The Cl^-–H_2, Br^-–H_2 and I^-–H_2 Dimers

3.1. *General*

The Cl^-–H_2, Br^-–H_2 and I^-–H_2 dimers are the simplest anion complexes to have been spectroscopically probed using the VP approach. At this stage they are the only anion complexes for which spectra exhibiting completely resolved rotational substructure have been obtained. Analysis of the spectra delivers quantitative information on the length and force constant of the intermolecular bonds as well as data on the rate at which vibrational energy, originally localized in the H–H stretch mode, is transferred to the weak intermolecular bond.

The halide–H_2 systems are appealing theoretical targets as they are small enough for accurate *ab initio* calculations of their potential energy surfaces. Equipped with a potential energy surface, it is possible to predict rotational and vibrational energy levels using approaches that go beyond the harmonic oscillator approximation. Comparing experimental and theoretical data for these simple systems allows one to choose an appropriate level of theory for treating more complicated negatively charged complexes and clusters for which high-resolution spectroscopic data are difficult to obtain, and for which theory remains the only route for predicting quantitative structural details.

The Cl^-–H_2, Br^-–H_2 and I^-–H_2 complexes are of wider significance because of their past and potential future roles as precursors in photoelectron and ZEKE studies aimed at investigating the potential energy surfaces of the benchmark halogen+H_2 triatomic rearrangement reactions [96]. Infrared spectra are a rich source of empirical data for testing and refining anion potential energy surfaces that are an important ingredient in theoretical simulations of the photoelectron spectra. So far, photoelectron studies have concentrated mainly on F^-–H_2 where photodetachment projects the system onto the transition state region of the $F+H_2 \rightarrow FH+H$ reaction potential energy surface [97, 98]. For many years this neutral reaction has served as a connection point between increasingly sophisticated scattering experiments, reaction dynamics theory and *ab initio* theory [96, 99]. Recent theoretical studies [100] suggest that photodetachment of the Cl^-–H_2 anion accesses a weak van der Waals minimum on the $Cl+H_2$ potential energy surface that has been implicated in influencing the HCl/DCl branching ratio in the Cl+HD reaction [101].

Like many of the hydrogen-bonded complexes listed in table 1, the halide–hydrogen complexes can be regarded as stabilized intermediates for simple acid-base proton transfer reactions:

$$H_2 + X^- \rightarrow H^- + HX. \qquad (1)$$

Since the proton affinity of H^- considerably exceeds those of Cl^-, Br^- and I^- (1675 versus 1395, 1354 and 1315 kJ mol^{-1} [102]), the complexes have X^-–H_2 ‘reactant-like’ forms. Schematic potential energy curves describing the proton transfer between

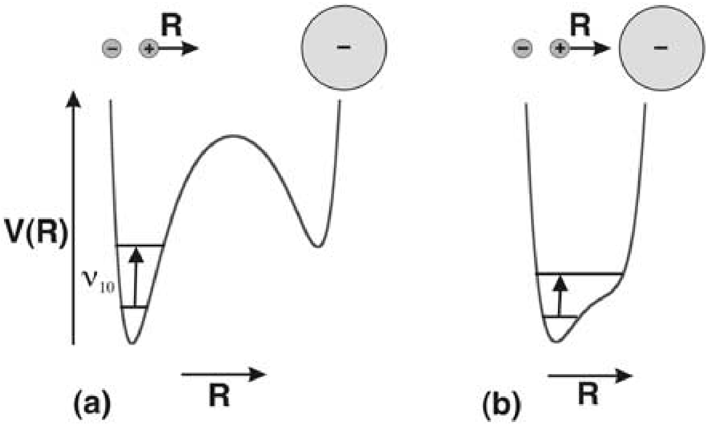

Figure 3. Schematic potential energy curves for a proton moving between hydride and halide anions. (*a*) For a large separation between H^- and X^- the potential curve has a double minimum corresponding to the two sides of the proton transfer reaction (equation (1)). (*b*) The potential curve has a single minimum for typical equilibrium separations of the X^-–H_2 complexes.

H^- and X^- are plotted in figure 3. For large H^-—X^- separations (figure 3(*a*)) the potential has two minima separated by a barrier, with the lower and upper minima corresponding respectively to reactant and product sides of equation (1). The barrier separating the minima disappears for H^-—X^- separations that are typical for the X^-–H_2 dimer (figure 3(*b*)). However, the intermediate proton's stretching potential is flatter than the stretching potential of the free H_2 molecule and as a consequence the frequency of the H_2 stretch vibration is reduced. The reduction in vibrational frequency scales with the proton affinity of the halide anion ($Cl^- > Br^- > I^-$).

3.2. *Infrared spectra*

The infrared spectra of the X^-–H_2 complexes are displayed in figure 4. The observed bands show the expected frequency shifts from the vibrational transition of the free H_2 molecule (which occurs at $\approx$4155 cm^{-1} for *ortho* H_2), in anticipation of the proton transfer reaction described in equation (1). The distinctive Σ–Σ structure of the bands (prominent P and R branches, absent Q branch) immediately suggests that the complexes possess linear equilibrium structures such that the H_2 molecule is hydrogen bonded to the halide ion. A linear geometry might be predicted from consideration of the interaction between the quadrupole moment of the H_2 molecule and the negatively charged halide anion.

Properties of the halide–H_2 dimers derived from the infrared spectra are summarized in table 2. Vibrationally averaged separations between the halide anion and the midpoint of the H–H bond for Cl^-–H_2, Br^-–H_2 and I^-–H_2, estimated from the rotational constants, are 3.20, 3.46 and 3.85 Å respectively. The harmonic force constants for the intermolecular bonds (derived from rotational and centrifugal distortion constants), which range from 1.3 $N\,m^{-1}$ for I^-–H_2 to 2.9 $N\,m^{-1}$ for Cl^-–H_2, are comparable with those for hydrogen-bonded neutral complexes (e.g. $k_s = 23.11\,N\,m^{-1}$ for HCN–HF [103]). The intermolecular bonds are rather long and weak compared with normal covalent bonds, reflecting the fact that the cohesion of the halide anion and the hydrogen molecule is due primarily to charge–quadrupole

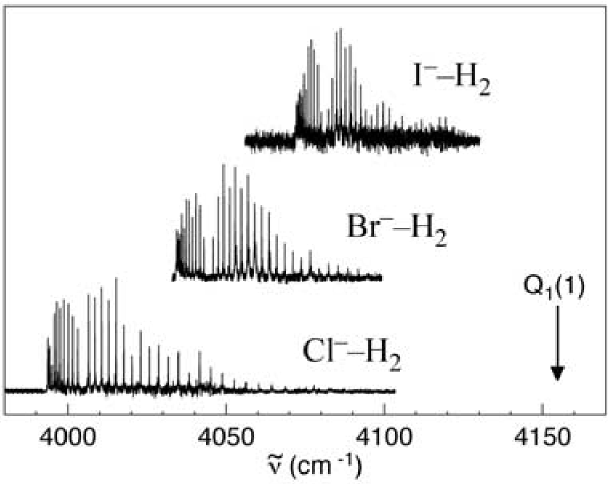

Figure 4. Infrared spectra of Cl^-–H_2, Br^-–H_2 and I^-–H_2 in the H–H stretch region. The bands, which are due to complexes containing *ortho* H_2, are shifted to lower frequency from the $Q_1(1)$ transition of *ortho* H_2 (marked by an arrow).

electrostatic and charge-induced-dipole induction interactions. The bonds of the isoelectronic LiCl, LiBr and LiI diatomic molecules are considerably shorter (2.02 [104], 2.17 [105] and 2.39 [106] Å), even when the extended nature of the H_2 subunit is taken into account.

Vibrational excitation of the H_2 molecule profoundly affects the X^-—H_2 intermolecular interaction. Spectroscopists will immediately recognize P-branch heads in the spectra shown in figure 4, indicating that the intermolecular bonds contract when the H_2 subunit is vibrationally excited. The contraction, which amounts to ≈0.1 Å for all three complexes, is accompanied by an increase in the stretching force constant for the intermolecular bond. The enhancement in the intermolecular bond strength is due mainly to a strengthening of the electrostatic and induction interactions arising from increases (≈10%) in the vibrationally averaged quadrupole moment and polarisability of the H_2 molecule when it is excited from the $v = 0$ to the $v = 1$ level [107].

The halide–H_2 complexes are rather floppy and even in the lowest vibrational level execute large amplitude excursions along the intermolecular stretching and bending coordinates. Particularly significant is the possibility for internal rotation of the H_2 molecule such that the bonding and terminal H atoms are exchanged. The situation is shown schematically in figure 5 where effective potential energy curves describing the intermolecular bending motion are presented. Because of the possibility of tunnelling between the two equivalent linear minima, each bending vibrational level is split into tunnelling doublets. The wavefunction of the lower level is symmetric (*s*) with respect to the tunnelling coordinate (θ) and corresponds to *para* H_2 interacting with the halide, while the upper-level wavefunction is antisymmetric (*a*) and corresponds to *ortho* H_2 interacting with the halide. Since the tunnelling barrier increases when the H_2 vibration is excited (mainly as a result of an increase in the H_2 quadrupole moment), the tunnelling splitting is reduced in the excited state. Therefore, the X^-–H_2 infrared spectra might be expected to consist of two sets of transitions (*s*–*s* and *a*–*a*) slightly displaced from one another.

Table 2. Data for halide–H_2 and halide–D_2 dimers (taken from [24–26]). Included are band origins (ν_o), band shifts from bare H_2 and D_2 stretching fundamentals ($\Delta\nu_o$), vibrationally averaged intermolecular separations (R_{cm}) and harmonic stretching force constants (k_s) for the intermolecular bond. Dissociation energies (D_o) and anharmonic stretching frequencies (ν_s) are estimated from Born–Oppenheimer (BO)–Rydberg–Klein–Rees (RKR) curves (see figure 7). Ground-state values ($v_{HH} = 0$ and $v_{DD} = 0$) are double primed, while excited state values ($v_{HH} = 1$ and $v_{DD} = 1$) have a single prime.

	$^{35}Cl^-$–$H_2(o)$	$^{35}Cl^-$–$D_2(o)$	$^{35}Cl^-$–$D_2(p)$	$^{81}Br^-$–$H_2(o)$	$^{79}Br^-$–$D_2(o)$	$^{79}Br^-$–$D_2(p)$	I^-–$H_2(o)$
ν_o (cm^{-1})	4004.84 (8)	2878.75 (8)	2878.51 (8)	4044.46 (8)	2907.46 (8)	2906.89 (8)	4081.11 (8)
$\Delta\nu_o$ (cm^{-1})^a	−150.4	−114.8	−113.0	−110.8	−86.1	−84.6	−74.1
R''_{cm} (Å)	3.195 (3)	3.159 (2)	3.159 (2)	3.461 (2)	3.414 (4)	3.413 (1)	3.851 (5)
R'_{cm} (Å)	3.077 (4)	3.081 (3)	3.081 (3)	3.346 (2)	3.339 (4)	3.337 (1)	3.739 (4)
k''_s (N m^{-1})	2.9 (1)	3.7 (3)	3.8 (3)	1.94 (5)	2.4 (7)	2.5 (1)	1.27 (9)
k'_s (N m^{-1})	3.8 (1)	4.5 (3)	4.6 (3)	2.64 (5)	3.2 (7)	3.1 (1)	1.68 (13)
ν''_s (cm^{-1})	151	127	129	123	98	101	97
ν_s (cm^{-1})	176	140	142	144	115	112	111
D''_o (cm^{-1})	488	499	559	365	364	418	253
D'_o (cm^{-1})	623	602	665	468	450	495	319

[a] Band shifts ($\Delta\nu_o$) for X^-–$H_2(o)$ are relative to the H_2 $Q_1(1)$ transition. Band shifts of X^-–$D_2(o)$ and X^-–$D_2(p)$ are relative to the D_2 $Q_1(0)$ and $Q_1(1)$ transitions.

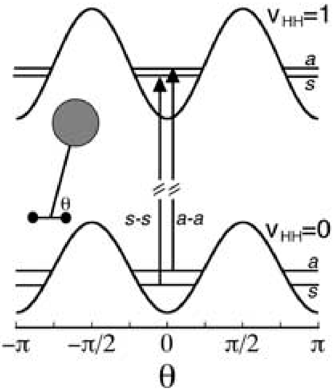

Figure 5. Angular potential energy curves for Cl^- interacting with H_2 with the diatomic in the $v_{HH} = 0$ (lower) and $v_{HH} = 1$ (upper) states. The height of the barrier increases on vibrational excitation of the H_2 molecule (mainly because of an increase in the H_2 quadrupole moment) leading to a decrease in the splitting between the lower symmetric (*s*) and upper antisymmetric (*a*) levels. For this reason the *a–a* transition occurs at slightly lower energy than the *s–s* transition. Neither the tunnelling splittings nor the separation between the lower and upper vibrational states is drawn to scale.

Surprisingly, only transitions due to complexes containing the *ortho* modification of H_2 are apparent in the X^-–H_2 spectra shown in figure 4. There are two reasons for this. Firstly, natural hydrogen gas consists of 25% *para* H_2 (even j) and 75% *ortho* H_2 (odd j). Secondly, complexes containing *ortho* H_2 are effectively bound by an additional $\approx 120\,\mathrm{cm}^{-1}$ compared with complexes containing *para* H_2. This comes about because the lowest dissociation limit for complexes containing *ortho* H_2 corresponds to H_2 ($j = 1$) fragments (with energy $2b_{HH} \approx 120\ \mathrm{cm}^{-1}$ above the ground state), while for complexes containing *para* H_2 the lowest dissociation limit corresponds to H_2 fragments in the $j = 0$ rotational state. For these reasons, any Cl^-–H_2 (*para*) complexes formed in the expansion are likely to be rapidly converted to Cl^-–H_2 (*ortho*) through the exothermic ligand exchange reaction:

$$Cl^-\text{–}H_2(para) + H_2(ortho) \rightarrow Cl^-\text{–}H_2(ortho) + H_2(para).$$

To explore this issue we have recorded spectra of the Cl^-–D_2 and Br^-–D_2 isotopomers. There should be a good chance of observing complexes containing both modifications of D_2 since the population ratio for the even and odd j levels is 2:1. Additionally, complexes containing *para* D_2 (odd j) are only bound by an additional $\approx 60\,\mathrm{cm}^{-1}$ compared with those containing *ortho* D_2 (even j). Indeed the spectrum of Cl^-–D_2, recorded in the region of the D–D stretch (figure 6), does display absorptions by Cl^-–D_2(*ortho*) and Cl^-–D_2(*para*), with the corresponding transitions separated by $0.24\,\mathrm{cm}^{-1}$. In the spectrum of the more weakly bound Br^-–D_2 dimer, the doubling is also observed, although the splitting is somewhat larger ($0.57\,\mathrm{cm}^{-1}$).

It is interesting to note that the harmonic force constants for the intermolecular stretching vibration for complexes containing H_2 are somewhat less than for those containing D_2. This is because the lighter H_2 molecule undergoes larger zero-point bending excursions than D_2, thereby sampling regions of the intermolecular potential energy surface where the charge-quadrupole interaction is less attractive than it is in the linear configuration (see figure 5).

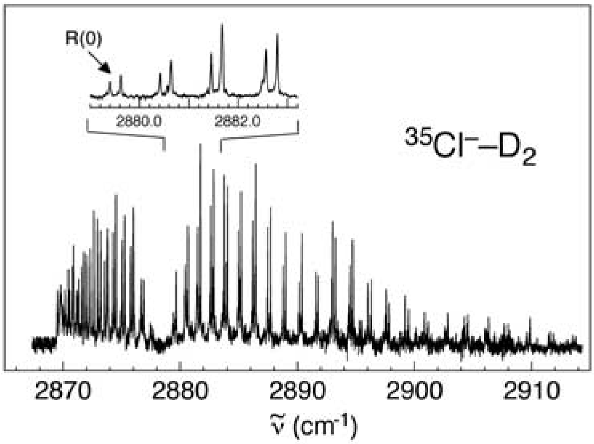

Figure 6. Infrared VP spectrum of $Cl^{-}–D_2$ in the D–D stretch region. Doubling ($\Delta = 0.24\,cm^{-1}$) due to the *s–s* and *a–a* transitions shown in figure 5 is clearly evident.

3.3. *Radial intermolecular potentials for halide–H_2 complexes*

The spectroscopic data have been used to develop effective radial potential energy curves for the halide–H_2 and halide–D_2 intermolecular interactions [24–26]. Near their minima, the potential curves are determined by RKR inversion of the spectroscopic data [108, 109]. At longer range, they are defined by the dominant electrostatic (charge–quadrupole) and induction (charge-induced dipole) potentials averaged over the hindered internal rotation of the H_2 subunit, assuming a BO-type separation between the intermolecular stretch vibration and the H–H stretch and intermolecular bend motions.

The BO–RKR curves for Cl^-, Br^- and I^- interacting with *ortho* H_2 ($v = 0$) are plotted together in figure 7. While at long range the curves are identical (this is a

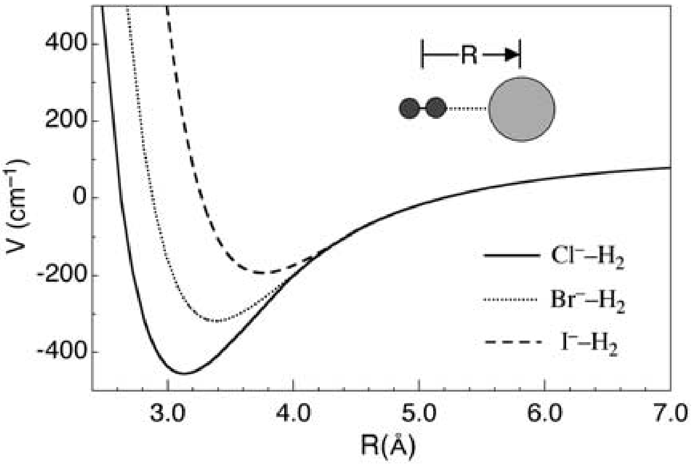

Figure 7. Radial intermolecular potential energy curves for the $Cl^-–H_2$, $Br^-–H_2$ and $I^-–H_2$ interactions. Near their minima, the potential curves are defined by RKR inversion of the spectroscopic data and at longer ranges by the halide—H_2 electrostatic and induction interactions.

consequence of their construction), they become noticeably shallower and have a larger equilibrium separation as the size of the halide ion increases. Dissociation energies and intermolecular stretching frequencies, estimated from the radial potential curves, are included in table 2. The dissociation energies for Cl^-–H_2 (*ortho*), Cl^-–D_2 (*ortho*) and Cl^-–D_2 (*para*) (488, 499, 559 cm^{-1}) are slightly lower than recently calculated values (527, 544, 604 [100]). It is likely that the BO–RKR dissociation energies may be slightly underestimated, since the long-range potentials do not include contributions from dispersion and higher-order electrostatic and induction interactions.

3.4. *Vibrational predissociation*

The strategy for obtaining the infrared spectra of the X^-–H_2 anion complexes relies on their dissociation into X^-+H_2 fragments after energy is deposited into the H–H stretch mode. The effectiveness of the strategy demonstrates that the complexes fragment on a timescale that is shorter than their flight time through the octopole region of the apparatus ($\approx$100 μs). There is evidence that the X^-–H_2 complexes predissociate quite rapidly; the widths of the rovibrational lines of Cl^-–H_2, Br^-–H_2 and I^-–H_2 exceed the bandwidth of the infrared light source (0.017 cm^{-1}), presumably because of lifetime broadening. By fitting the lines with Voigt profiles, with the width of the Gaussian component fixed to the bandwidth of the OPO (0.017 cm^{-1}), the widths of the Lorentzian components were estimated as 0.032 ± 0.005 cm^{-1} (Cl^-–H_2), 0.021 ± 0.006 cm^{-1} (Br^-–H_2) and 0.016 ± 0.007 cm^{-1} (I^-–H_2). These widths correspond to predissociation lifetimes of 165, 250 and 330 ps respectively. It is interesting to note that the predissociation rates, which decrease in the order Cl^-–H_2>Br^-–H_2>I^-–H_2, diminish with the strength of the intermolecular bonds, and presumably with the strength of the coupling between the H–H stretch mode and the intermolecular coordinate. Linewidths for Cl^-–D_2 and Br^-–D_2 are close to the bandwidth of the OPO light source, indicating that VP lifetimes for these two complexes exceed 500 ps.

4. Anions in the Interior: Halide–Acetylene Clusters

4.1. *General*

To explore the manner in which a halide anion is progressively solvated by larger molecules we have obtained infrared spectra of the Cl^-–$(C_2H_2)_n$ and Br^-–$(C_2H_2)_n$ clusters containing up to nine acetylene ligands. Although generally the spectra are not rotationally resolved, inferences can be drawn regarding the clusters' structures since the local environment of the C_2H_2 ligands is reflected by the frequencies and intensities of the C–H stretch vibrations. The principal structural diagnostic is the frequency of the acetylene ν_3 antisymmetric C–H stretching vibration, which occurs at 3288.7 cm^{-1} for the free C_2H_2 molecule. Acetylene molecules that are hydrogen bonded to the halide anion have large ν_3 frequency shifts, while acetylene molecules that are situated further from the anion exhibit ν_3 absorptions that are much closer to that of the free C_2H_2 molecule.

4.2. *The Br^-–C_2H_2 dimer*

We begin by discussing the VP spectrum of the Br^-–C_2H_2 dimer (figure 8). The most intense band spans the 2970–3060 cm^{-1} range, well below the ν_3 transition of

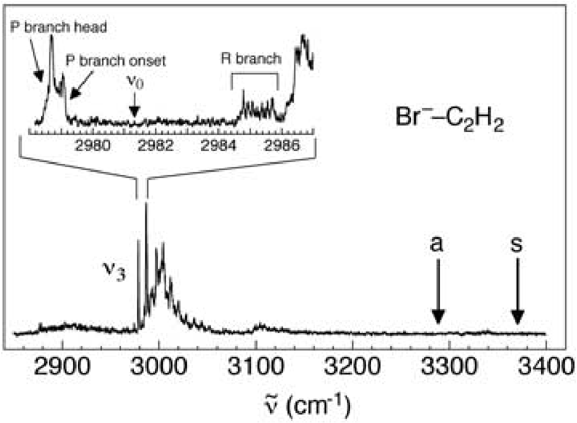

Figure 8. Infrared VP spectrum of the Br^-–C_2H_2 dimer over the 2850–3400 cm^{-1} range, obtained by monitoring Br^- fragment ion. The arrows labelled 's' and 'a' mark the positions of the C_2H_2 ν_1 (symmetric C–H stretch) and ν_3 (antisymmetric C–H stretch) vibrations. The inset is an expanded view of the region covering the two lowest-energy sharp peaks in the spectrum. The feature to lowest energy is the ν_3 P-branch head. Lower J lines in the P and R branches are missing because the upper levels lie below the dissociation threshold.

free acetylene, and comprises a series of sharp peaks protruding from a broad hump. This band can be convincingly associated with the ν_3 transition of a linear Br^-–HCCH complex, shifted to lower frequency by virtue of the interaction between the hydrogen-bonded proton and the Br^- anion. The peak to lowest frequency has a sharp onset, consistent with its assignment as the P-branch head of the Br^-–C_2H_2 ν_3 transition. The spiked peak structure extending from the lowest energy peak out to 3060 cm^{-1} is a series of hot bands of the type $(\nu_3 + m\nu_s + n\nu_b) \leftarrow (m\nu_s + n\nu_b)$, where ν_s and ν_b are the intermolecular stretching and bending modes. The formation of a head in the P branch of the ν_3 transition, along with the blue-shifted hot bands, implies that a shortening and stiffening of the intermolecular bond accompanies stretching excitation of the shared proton. This is a general feature of proton-bound ionic complexes and has been observed in both cation and anion systems [16, 87, 110].

Figure 8 shows an expanded view of the Br^-–C_2H_2 spectrum in the vicinity of the two lowest energy sharp peaks. The structure is curious. To lower energy there is an isolated band head (at 2978.7 cm^{-1}), while at higher energy there are seven narrow lines occurring before the onset of the next band head. The lines have widths that are of the order of the OPO bandwidth (0.017 cm^{-1}) and are due to resolved rovibrational transitions. The most convincing explanation for the odd structure is that onset of dissociation occurs at a specific upper-state rotational energy level and that the lower J lines in the P and R branches are absent from the VP spectrum because the upper levels lie below the dissociation threshold. The band origin ($\nu_o = 2981.28$ cm^{-1}) and rotational constants ($B'' = 0.0488$ cm^{-1}, $\Delta B = 9.3 \times 10^{-4}$ cm^{-1}) were ascertained by fitting the observed features to a pseudodiatomic Σ–Σ energy level expression. The frequency of the ν_3 band compares very well with a recent theoretical estimate based on large-scale CCSD(T) calculations (2964 cm^{-1}) [62].

The commencement of dissociation at a specific J' level in the ν_3 rovibrational manifold allows the Br^-—HCCH bond dissociation energy to be estimated as $D_0 = 3020 \pm 3\ cm^{-1}$. To date, this probably represents the most accurately determined dissociation energy for an anion complex and compares very well with recent theoretical estimates [62].

4.3. *Larger Br^-–$(C_2H_2)_n$ clusters*

What happens as more acetylene molecules are added to form larger clusters? Infrared VP spectra of mass-selected Br^-–$(C_2H_2)_n$ clusters with $1 \leq n \leq 8$ are shown in figure 9. For clusters containing up to six acetylene molecules the spectra remain relatively simple, each being dominated by a single peak that shifts progressively back towards the frequency of the ν_3 vibration of the free acetylene molecule. These observations constitute evidence that a central Br^- core is surrounded by equivalent, hydrogen-bonded C_2H_2 ligands, with the bromide–acetylene bonds becoming progressively weaker with increasing cluster size. Structures that are consistent with the infrared spectra are shown in figure 10. The disposition of the C_2H_2 entities in the larger Br^-–$(C_2H_2)_n$ clusters reflects the dominant long-range charge–quadrupole electrostatic interaction between the halide anion and the acetylene molecules which favours linear Br^-—HCCH intermolecular bonds. At the same time, repulsive quadrupole–quadrupole interactions should tend to ensure that the acetylene ligands are separated from one another. The clusters are probably highly fluxional, particularly in coordinates corresponding to angular motion of the acetylene units about the Br^- core.

Steric crowding limits the number of C_2H_2 ligands that can be accommodated in the inner solvation shell. Indeed there is evidence that acetylene ligands begin to occupy the second solvation shell for clusters larger than Br^-–$(C_2H_2)_6$. Expanded

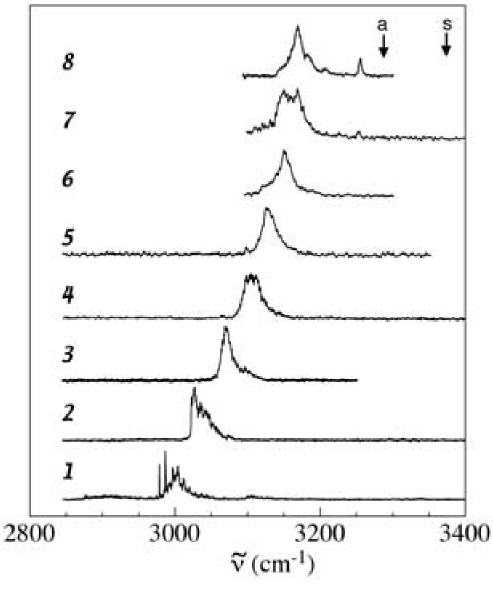

Figure 9. Infrared VP spectra of Br^-–$(C_2H_2)_n$ ($1 \leq n \leq 8$) anion complexes over the 2850–3450 cm^{-1} range. The arrows labelled 's' and 'a' mark the positions of the C_2H_2 ν_1 and ν_3 vibrations.

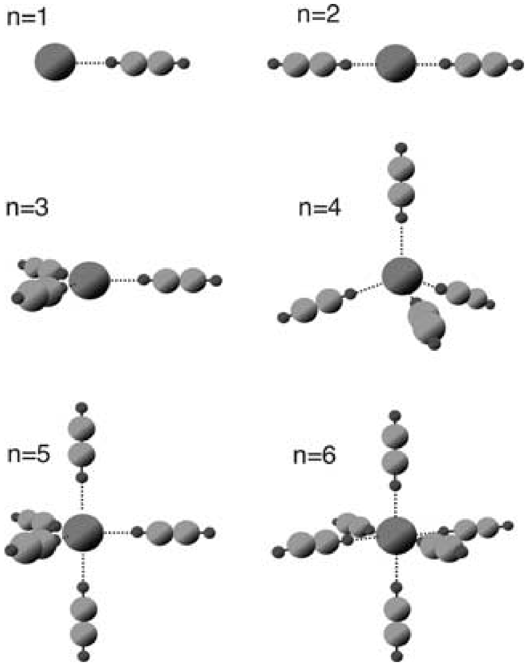

Figure 10. Proposed structures for the Br^-–$(C_2H_2)_n$ ($n = 1$–6) complexes.

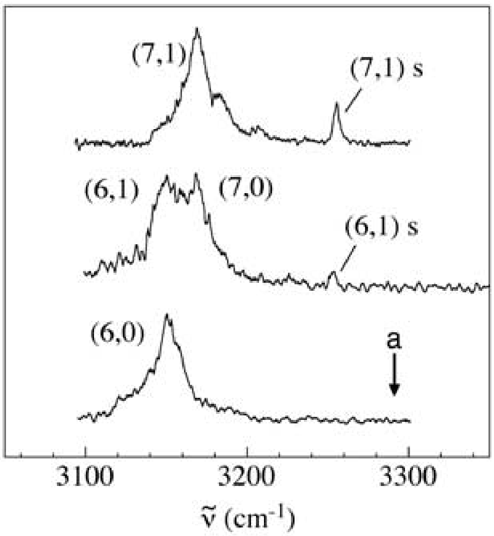

Figure 11. Infrared spectra of the Br^-–$(C_2H_2)_n$ ($n = 6$–8) complexes. The arrow labelled 'a' marks the position of the free C_2H_2 ν_3 band. The bands labelled with an 's' are due to acetylene molecules in the second solvation shell.

views of Br^-–$(C_2H_2)_6$, Br^-–$(C_2H_2)_7$ and Br^-–$(C_2H_2)_8$ spectra are displayed in figure 11. In addition to the dominant peak associated with the inner solvation shell C_2H_2 subunits there is, in the spectra of Br^-–$(C_2H_2)_7$ and Br^-–$(C_2H_2)_8$, a weak, narrow band red shifted by only 34 cm^{-1} from the ν_3 vibration of the free acetylene

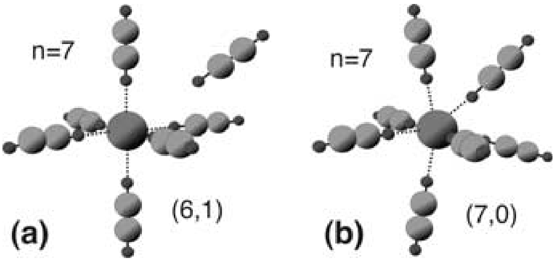

Figure 12. Two proposed isomers for the $Br^-–(C_2H_2)_7$ cluster.

molecule. This additional band is characteristic of an acetylene molecule interacting less strongly with the Br^- ion core which is likely to be situated in the second solvation shell. A possible structure for the $n = 7$ cluster, with six acetylenes in the first solvation shell, and one acetylene in the second solvation shell, is shown in figure 12(*a*). The dominant cohesive forces for the acetylene molecule in the second shell should still arise from charge–quadrupole and induction interactions with the central Br^-. This, together with the fact that the acetylene–acetylene interaction potential favours a slipped parallel arrangement for the acetylene dimer [111], makes it likely that the second shell ligand slips between inner shell acetylenes while being prevented from making intimate contact with the halide anion core owing to steric crowding.

There is also evidence for a second $Br^-–(C_2H_2)_7$ isomer in which all seven ligands are bound directly to the halide anion core (figure 12(*b*)). The main indication for this comes from the fact that the more intense band in the $Br^-–(C_2H_2)_7$ spectrum is split into two components. The lower-energy component occurs at the same frequency as the $Br^-–(C_2H_2)_6$ absorption and is assigned to the (6,1) isomer, with six C_2H_2 ligands in the first solvation shell and one ligand in the second solvation shell. The frequency of the higher-energy component can be anticipated by extrapolating the ν frequencies of the $n = 1–6$ complexes, and is assigned to the (7,0) isomer in which all seven ligands occupy first solvation shell sites. The main ν_3 band in the $Br^-–(C_2H_2)_8$ spectrum consists of a single peak at the same frequency as the ν_3 band of the $Br^-–(C_2H_2)_7$ (7,0) isomer, suggesting the predominance of a single (7,1) isomeric form for $n = 8$.

Corresponding infrared spectra of $Cl^-–(C_2H_2)_n$ ($1 \leq n \leq 9$) and $I^-–(C_2H_2)_n$ ($1 \leq n \leq 4$) clusters [16, 41] show that they too adopt interior solvation structures in which the halide is surrounded by hydrogen-bonded C_2H_2 ligands. There is evidence that the second solvation shell is initiated at a slightly later stage for $Cl^-–(C_2H_2)_n$ than it is for $Br^-–(C_2H_2)_n$. The difference may be due to the fact that the Cl^-—HCCH bonds are somewhat stronger than the Br^-—HCCH bonds.

The appearance of spectroscopically distinguishable isomers for the larger halide–acetylene complexes raises intriguing questions. For example, does the $Br^-–(C_2H_2)_n$ beam contain populations of non-interconverting (7,0) and (6,1) isomers or does dynamical interconversion occur? If the latter is true, how rapidly does the isomerization happen? Perhaps some of these questions can be addressed through hole burning experiments, whereby one infrared beam is fixed to a resonance characteristic of one isomer (such as the peak associated with the second-shell C_2H_2 ligand) while a second tuneable infrared beam is scanned over the band.

5. Outlook

Exciting opportunities remain for extending spectroscopic investigations of negatively charged complexes and clusters in the gas phase. A host of anion complexes observed in mass spectrometric and photoelectron studies have yet to be probed in the infrared. Many chemically significant complexes such as $F^-–H_2O$, $Cl^-–H_2O$, $Br^-–H_2O$ and $OH^-–H_2O$ are too strongly bound for high-resolution study using the VP technique so that other strategies must be sought to probe their structures. As mentioned earlier, very significant progress has been made in spectroscopically characterizing these species by attaching easily dislodged 'spy' atoms. The problem with this approach is that it does not yield high-resolution spectroscopic data for the core anion complex. On the positive side, the relatively strong intermolecular bonds in these complexes may favour their formation in sufficient abundances for investigation using traditional spectroscopic techniques such as direct infrared absorption in electron-impact-excited supersonic plasmas. This route that has been profitably deployed to obtain spectra of several cation complexes including N_4^+ [112] and $Ar–HN_2^+$ [113].

Other interesting anion complexes and clusters await investigation through spectroscopic studies. For example, dianion clusters such as $SO_4^{2-}–(H_2O)_n$, which can be introduced into the gas phase using electrospray ion sources, have recently been explored in photoelectron studies [114]. The bare SO_4^{2-} dianion is unstable in the gas phase owing to Coulomb repulsion, and at least three water molecules are required for its stabilization. It remains to be seen whether infrared VP spectroscopy can be deployed to provide information on the vibrational frequencies of this and other doubly charged anion clusters.

Dipole-bound anion complexes and clusters are another exotic class of anion clusters that have been characterized in photoelectron and electron attachment investigations, yet have received limited attention through infrared spectroscopic studies. In these delicate species, which include $(H_2O)_2^-$ [115], $(H_2O–NH_3)^-$ [116] and $(HF)_2^-$ [117], the electron is bound by electrostatic interaction with the dipole moment of the cluster core (which needs to exceed 2.5 D) and exists in a diffuse orbital that extends well beyond the molecular framework. To date the only infrared spectroscopic investigations of these fascinating species have been of the $(H_2O)_n^-$ hydrated electron clusters by Johnson and coworkers, with the available experimental and theoretical data suggesting that the $n = 5–11$ clusters are linear 'chain-like' species [56].

The predissociation dynamics of ionic complexes and clusters also deserves more attention. While in a few instances the widths of rotationally resolved transitions provide information on the predissociation rate, little is known about how the available energy is partitioned into translational, rotational and vibrational degrees of freedom of the neutral and charged fragments. In principle, much could be learned by measuring the fragments' translational energy distribution in a fast ion beam apparatus. Such studies would be particularly informative for the halide–H_2 and halide–D_2 dimers where any excess energy is partitioned between the H_2 (D_2) rotational motion and relative translation motion.

Acknowledgments

We are grateful to the Australian Research Council and the University of Melbourne for supporting our laboratory investigations of anion complexes and clusters.

References

[1] Legon, A. C., 1983, *Ann. Rev. phys. Chem.*, **34**, 275.

[2] Nesbitt, D. J., 1988, *Chem. Rev.*, **88**, 843.

[3] Hutson, J. M., 1990, *Ann. Rev. phys. Chem.*, **41**, 123.

[4] Heaven, M. C., 1992, *Ann. Rev. phys. Chem.*, **42**, 283.

[5] Elrod, M. J., and Saykally, R. J., 1994, *Chem. Rev.*, **94**, 1975.

[6] Leopold, K. R., Fraser, G. T., Novick, S. E., and Klemperer, W., 1994, *Chem. Rev.*, **94**, 1807.

[7] Bacic, Z., and Miller, R. E., 1996, *J. phys. Chem.*, **100**, 12945.

[8] Zwier, T. S., 1996, *Ann. Rev. phys. Chem.*, **47**, 205.

[9] Four special issues of *Chem. Rev.* (1986, **86**(3); 1988, **88**(6); 1994, **94**(7); 2000, **100**(11)) are devoted to van der Waals complexes and clusters.

[10] Okumura, M., Yeh, L. I., and Lee, Y. T., 1985, *J. chem. Phys.*, **83**, 3705.

[11] Okumura, M., Yeh, L. I., Myers, J. D., and Lee, Y. T., 1986, *J. chem. Phys.*, **85**, 2328.

[12] Liu, W. L., and Lisy, J. M., 1988, *J. chem. Phys.*, **89**, 605.

[13] Johnson, M. S., Kuwata, K. T., Wong, C.-K., and Okumura, M., 1996, *Chem. Phys. Lett.*, **260**, 551.

[14] Bailey, C. G., Kim, J., Dessent, C. E. H., and Johnson, M. A., 1997, *Chem. Phys. Lett.*, **269**, 122.

[15] Cabarcos, O. M., Weinheimer, C. J., Lisy, J. M., and Xantheas, S. S., 1999, *J. chem. Phys.*, **110**, 5.

[16] Weiser, P. S., Wild, D. A., and Bieske, E. J., 1999, *Chem. Phys. Lett.*, **299**, 303.

[17] Kebarle, P., 1975, *NATO Adv. Study Inst. Ser.* B, **B6**, 459.

[18] Kebarle, P., 1977, *Annu. Rev. phys. Chem.*, **28**, 445.

[19] Castleman, A. W., and Keesee, R. G., 1986, *Chem. Rev.*, **86**, 589.

[20] Meot-Ner, M. M., and Lias, S. G., 2001, *NIST Chemistry WebBook, NIST Standard Reference Database Number 69*, edited by P. J. Linstrom and W. G. Mallard (Gaithersburg, MD: National Institute of Standards and Technology) (http://webbook.nist.gov).

[21] Meot-Ner, M., and Speller, C. V., 1986, *J. phys. Chem.*, **90**, 6616.

[22] Wild, D. A., Weiser, P. S., Loh, Z. M., and Bieske, E. J., 2002, *J. phys. Chem.* A, **106**, 906.

[23] Wild, D. A., Wilson, R. L., Weiser, P. S., and Bieske, E. J., 2000, *J. chem. Phys.*, **113**, 10154.

[24] Wild, D. A., Weiser, P. S., Bieske, E. J., and Zehnacker, A., 2001, *J. chem. Phys.*, **115**, 824.

[25] Wild, D. A., Weiser, P. S., and Bieske, E. J., 2001, *J. chem. Phys.*, **115**, 6394.

[26] Wild, D. A., Loh, Z. M., Wilson, R. L., and Bieske, E. J., 2002, *J. chem. Phys.*, **117**, 3256.

[27] Ayotte, P., Nielsen, S. B., Weddle, G. H., Johnson, M. A., and Xantheas, S. S., 1999, *J. phys. Chem.* A, **103**, 10665.

[28] Choi, J.-H., Kuwata, K. T., Cao, Y.-B., and Okumura, M., 1998, *J. phys. Chem.* A, **102**, 503.

[29] Ayotte, P., Weddle, G. H., Kim, J., and Johnson, M. A., 1998, *J. Am. Chem. Soc.*, **120**, 12361.

[30] Ayotte, P., Weddle, G. H., and Johnson, M. A., 1999, *J. chem. Phys.*, **110**, 7129.

[31] Kelley, J. A., Weber, J. M., Lisle, K. M., Robertson, W. H., Ayotte, P., and Johnson, M. A., 2000, *Chem. Phys. Lett.*, **327**, 1.

[32] Corcelli, S. A., Kelley, J. A., Tully, J. C., and Johnson, M. A., 2002, *J. phys. Chem.* A, **106**, 4872.

[33] Ayotte, P., Bailey, C. G., and Johnson, M. A., 1998, *J. phys. Chem.* A, **102**, 3067.

[34] Ayotte, P., Bailey, C. G., Weddle, G. H., and Johnson, M. A., 1998, *J. phys. Chem.*, **102**, 3067.

[35] Ayotte, P., Weddle, G. H., Kim, J., and Johnson, M. A., 1998, *Chem. Phys.*, **239**, 485.

[36] Ayotte, P., Weddle, G. H., Kim, J., Kelley, J., and Johnson, M. A., 1999, *J. phys. Chem.* A, **103**, 443.

[37] Weber, J. M., Kelley, J. A., Nielsen, S. B., Ayotte, P., and Johnson, M. A., 2000, *Science*, **287**, 2461.

[38] Weber, J. M., Kelley, J. A., Robertson, W. H., and Johnson, M. A., 2001, *J. chem. Phys.*, **114**, 2698.

[39] Chaudhuri, C., Wang, Y.-S., Jiang, J. C., Lee, Y. T., Chang, H.-C., and Niedner-Schatteburg, G., 2001, *Mol. Phys.*, **99**, 1161.

[40] Woronowicz, E. A., Robertson, W. H., Weddle, G. H., Johnson, M. A., Myshakin, E. M., and Jordan, K. D., 2002, *J. phys. Chem.* A, **106**, 7086.

[41] Weiser, P. S., Wild, D. A., and Bieske, E. J., 1999, *J. chem. Phys.*, **110**, 9443.

[42] Wild, D. A., Milley, P. J., Loh, Z. M., Weiser, P. S., and Bieske, E. J., 2000, *Chem. Phys. Lett.*, **323**, 49.

[43] Wild, D. A., Milley, P. J., Loh, Z. M., Wolynec, P. P., Weiser, P. S., and Bieske, E. J., 2000, *J. chem. Phys.*, **113**, 1075.

[44] Weiser, P. S., Wild, D. A., Wolynec, P. P., and Bieske, E. J., 2000, *J. phys. Chem.* A, **104**, 2562.

[45] Nielsen, S. B., Ayotte, P., Kelley, J. A., Weddle, G. H., and Johnson, M. A., 1999, *J. chem. Phys.*, **111**, 10464.

[46] Wild, D. A., Loh, Z. M., and Bieske, E. J., 2002, *Int. J. Mass Spectrom.*, **220**, 273.

[47] Wild, D. A., Loh, Z. M., Wolynec, P. P., Weiser, P. S., and Bieske, E. J., 2000, *Chem. Phys. Lett.*, **332**, 531.

[48] Robertson, W. H., Kelley, J. A., and Johnson, M. A., 2000, *J. chem. Phys.*, **113**, 7879.

[49] Cabarcos, O. M., Weinheimer, C. J., Martinez, T. J., and Lisy, J. M., 1999, *J. chem. Phys.*, **110**, 9516.

[50] Nielsen, S. B., Ayotte, P., Kelley, J. A., and Johnson, M. A., 1999, *J. chem. Phys.*, **111**, 9593.

[51] Robertson, W. H., Karapetian, K., Ayotte, P., Jordan, K. D., and Johnson, M. A., 2002, *J. chem. Phys.*, **116**, 4853.

[52] Ayotte, P., Kim, J., Kelley, J. A., Nielsen, S. B., and Johnson, M. A., 1999, *J. Am. Chem. Soc.*, **121**, 6950.

[53] Ichihashi, M., Sadanaga, Y., Lisy, J. M., and Kondow, T., 2000, *Chem. Lett.*, 1240.

[54] Bailey, C. G., Kim, J., and Johnson, M. A., 1996, *J. phys. Chem.*, **100**, 16782.

[55] Ayotte, P., Bailey, C. G., Kim, J., and Johnson, M. A., 1998, *J. chem. Phys.*, **108**, 444.

[56] Ayotte, P., Weddle, G. H., Bailey, C. G., Johnson, M. A., Vila, F., and Jordan, K. D., 1999, *J. chem. Phys.*, **110**, 6268.

[57] Xantheas, S. S., 1996, *J. phys. Chem.*, **100**, 9703.

[58] Boldyrev, A. I., Simons, J., Mil'nikov, G. V., Benderskii, V. A., Grebenshchikov, S. Y., and Vetoshkin, E., 1995, *J. chem. Phys.*, **102**, 1295.

[59] Xantheas, S. S., and Dunning, T. H., 1994, *J. phys. Chem.*, **98**, 13489.

[60] Xantheas, S., 1995, *J. Am. Chem. Soc.*, **117**, 10373.

[61] Botschwina, P., Dutoi, T., Mladenovic, M., Oswald, R., Schmatz, S., and Stoll, H., 2001, *Faraday Discuss.*, **118**, 433.

[62] Botschwina, P., and Stoll, H., 2001, *Phys. Chem. chem. Phys.*, **3**, 1965.

[63] Gutowski, M., Skurski, P., Jordan, K. D., and Simons, J., 1997, *Int. J. quant. Chem.*, **64**, 183.

[64] Combariza, J. E., Kestner, N. R., and Jortner, J., 1994, *J. chem. Phys.*, **100**, 2851.

[65] Simons, J., and Jordan, K. H., 1987, *Chem. Rev.*, **87**, 535.

[66] Johnson, M., and Lineberger, W. C., 1988, *Techniques for the Study of Ion-Molecule Reactions*, Vol. XX, 591, edited by J. M. Farrar and W. H. J. Saunders (New York: Wiley).

[67] Castleman Jr, A. W., and Bowen Jr, K. H., 1996, *J. phys. Chem.*, **100**, 12911.

[68] Markovich, G., Perera, L., Berkowitz, M. L., and Cheshnovsky, O., 1996, *J. chem. Phys.*, **105**, 2675.

[69] Arnold, S. T., Hendricks, J. H., and Bowen, K. H., 1995, *J. chem. Phys.*, **102**, 39.

[70] Neumark, D. M., 1992, *Annu. Rev. phys. Chem.*, **43**, 153.

[71] Neumark, D. M., 1993, *Acc. chem. Res.*, **26**, 33.

[72] Neumark, D. M., 1996, *Science*, **272**, 1446.

[73] Boesl, U., and Knott, W. J., 1999, *Mass Spectrom. Rev.*, **17**, 275.

[74] Lenzer, T., Yourshaw, I., Furlanetto, M. R., Reiser, G., and Neumark, D. M., 1999, *J. chem. Phys.*, **110**, 9578.

[75] Yourshaw, I., Lenzer, T., Reiser, G., and Neumark, D. M., 1998, *J. chem. Phys.*, **109**, 5247.

[76] Vorsa, V., Nandi, S., Campagnola, P. J., Larsson, M., and Lineberger, W. C., 1997, *J. chem. Phys.*, **106**, 1402.

[77] Sanov, A., Faeder, J., Parson, R., and Lineberger, W. C., 1999, *Chem. Phys. Lett.*, **313**, 812.

[78] Greenblatt, B. J., Zanni, M. T., and Neumark, D. M., 1999, *J. chem. Phys.*, **111**, 10566.

[79] Greenblatt, B. J., Zanni, M. T., and Neumark, D. M., 2000, *J. chem. Phys.*, **112**, 601.

[80] Weber, J. M., Leber, E., Ruf, M. W., and Hotop, H., 1999, *Eur. phys. J. D*, **7**, 587.

[81] Desfrancois, C., Lisfi, A., and Schermann, J. P., 1992, *Z. Phys.* D, **24**, 297.

[82] Nizkorodov, S. A., Dopfer, O., Ruchti, T., Meuwly, M., Maier, J. P., and Bieske, E. J., 1995, *J. phys. Chem.*, **99**, 17118.

[83] McGillvery, D. C., and Morrison, J. D., 1977, *J. chem. Phys.*, **67**, 368.

[84] Dunbar, R. C., 2000, *Int. J. Mass Spectrom.*, **200**, 571.

[85] Carrington, A., 1996, *Science*, **274**, 1327.

[86] Crofton, M. W., Price, J. M., and Lee, Y. T., 1994, *Springer Ser. chem. Phys.*, **56**, 44.

[87] Bieske, E. J., and Dopfer, O., 2000, *Chem. Rev.*, **100**, 3963.

[88] Weinheimer, C. J., and Lisy, J. M., 1996, *J. chem. Phys.*, **105**, 2938.

[89] Lisy, J. M., 1997, *Int. Rev. phys. Chem.*, **16**, 267.

[90] Gregoire, G., and Duncan, M. A., 2002, *J. chem. Phys.*, **117**, 2120.

[91] Miyazaki, M., Fujii, A., Ebata, T., and Mikami, N., 2001, *Chem. Phys. Lett.*, **349**, 431.

[92] Solca, N., and Dopfer, O., 2001, *J. phys. Chem.* A, **105**, 5637.

[93] Yeh, L. I., Okumura, M., Myers, J. D., Price, J. M., and Lee, Y. T., 1989, *J. chem. Phys.*, **91**, 7319.

[94] Takasu, R., Hashimoto, K., and Fuke, K., 1996, *Chem. Phys. Lett.*, **258**, 94.

[95] Boesl, U., Bassmann, C., Drechsler, G., and Distelrath, V., 1999, *Eur. J. Mass Spectrom.*, **5**, 455.

[96] Neumark, D. M., 2002, *PhysChemCom*, **5**, 76.

[97] Weaver, A., and Neumark, D. M., 1991, *Faraday Discuss. Chem. Soc.*, **91**, 5.

[98] Manolopoulos, D. E., Stark, K., Werner, H. J., Arnold, D. W., Bradforth, S. E., and Neumark, D. M., 1993, *Science*, **262**, 1852.

[99] Levine, R. D., and Bernstein, R. B., 1987, *Molecular Reaction Dynamics and Chemical Reactivity* (New York: Oxford University Press).

[100] Alexander, M., 2002, personal communication.

[101] Skouteris, D., Manalopolous, D. E., Bian, W. S., Werner, H. J., Lai, L. H., and Liu, K., 1999, *Science*, **296**, 1713.

[102] Lias, S. G., Barmess, J. E., Liebman, J. F., Holmes, J. L., Levin, R. D., and Mallard, W. G., 1988, *J. phys. Chem. Ref. Data Suppl.*, **17**, 1.

[103] Bevan, J. W., 1987, *Structure and Dynamics of Weakly Bound Molecular Complexes*, NATO ASI Series, Vol. 212, 149, edited by A. Weber (Dordrecht: Reidel).

[104] Pearson, E. F., and Gordy, W., 1969, *Phys. Rev.*, **177**, 52.

[105] Hebert, A. J., Breivogel Jr, F. W., and Street Jr, K., 1964, *J. chem. Phys.*, **41**, 2368.

[106] Breivogel Jr, F. W., Hebert, A. J., and Street Jr, K., 1965, *J. chem. Phys.*, **42**, 1555.

[107] Hunt, J. L., Poll, J. D., and Wolniewicz, L., 1984, *Can. J. Phys.*, **62**, 1719.

[108] Child, M. S., and Nesbitt, D. J., 1988, *Chem. Phys. Lett.*, **149**, 404.

[109] Nesbitt, D. J., Child, M. S., and Clary, D. C., 1989, *J. chem. Phys.*, **90**, 4855.

[110] Nizkorodov, S. A., Maier, J. P., and Bieske, E. J., 1995, *J. chem. Phys.*, **102**, 5570.

[111] Fraser, G. T., Suenram, R. D., Lovas, F. J., Pine, A. S., Hougen, J. T., Lafferty, W. J., and Muenter, J. S., 1988, *J. chem. Phys.*, **89**, 6028.

[112] Ruchti, T., Speck, T., Connelly, J. P., Bieske, E. J., Linnartz, H., and Maier, J. P., 1996, *J. chem. Phys.*, **105**, 2591.

[113] Speck, T., Linnartz, H., and Maier, J. P., 1997, *J. chem. Phys.*, **107**, 8706.

[114] Yang, X., Wang, X.-B., and Wang, L.-S., 2002, *J. phys. Chem.* A, **106**, 7607.

[115] Lee, G. H., Arnold, S. T., Eaton, J. G., Sarkas, H. W., Bowen, K. H., Ludewigt, C., and Haberland, H., 1991, *Z. Phys.* D, **20**, 9.

[116] Abdoul-Carime, H., Wakisaka, A., Bouteiller, Y., Desfrancois, C., and Schermann, J. P., 1997, *Z. Phys.* D, **40**, 55.

[117] Hendricks, J. H., de Clercq, H. L., Lyapustina, S. A., and Bowen Jr, K. H., 1997, *J. chem. Phys.*, **107**, 2962.